RESEARCH ARTICLE   OPEN ACCESS

Three-Phase Nine-Level Inverter for Photovoltaic System with Induction Motor

A R Neelakanteswara Rao[1], T Nagadurga[2]
[1]*M.TECH Scholar, Dept of EEE, GEC Gudlavalleru, AP, India*
[2]*Assistant Professor, Dept. of EEE, GEC Gudlavalleru, AP, India*

Abstract
Electrical power play a vital rule in 21th century, but non-conventional sources scale down day by day. Not only that concern for the environmental pollution around the world, so now a day's photovoltaic (PV) power systems are getting more and more widespread with the increase in the energy demand. This paper proposed a three phase nine level inverter with voltage control method using semiconductor power devices for three phase induction motor in order to achieve a smooth, continuous and low total harmonics distortion (THD) waveforms. The proposed inverter system gives better voltage regulation, smooth results and efficiency compared to multi-level inverters. The inverter is capable of producing nine levels of output voltage levels (V_{dc}, $3V_{dc}/4$, $V_{dc}/2$, $V_{dc}/4$, 0, $-V_{dc}/4$, $-V_{dc}/2$, $-3V_{dc}/4$, $-V_{dc}$) The proposed inverter was verified by using simulation of MATLAB/SIMULINK software.

Index terms: Photovoltaic (PV) system, multi-level inverter, semiconductor power devices, THD, induction motor.

I.   Introduction

As the world is concerned with the fossil fuel exhaustion and environmental problem caused by conventional power generation, particularly solar have become very popular and demanding. PV sources are used in many applications because they have advantage of being maintenance and pollution free. It is used to convert the dc power from solar module to ac power to feed into load.

The proposed three phase nine level inverter is very suitable to PV module with induction motor load, because of compare to common three phase multi-level inverter have high switching, but it could also unfortunately increase switching losses, acoustic noise, and level of interference to other equipment. Improving its output waveform reduces its harmonic content and, hence, also the size of the filter used and the level of electromagnetic interference (EMI) generated by the inverter's switching operation.

This paper developed a modified H-bridge single-phase multilevel inverter that has two diode embedded bidirectional switches. Coming to three phase proposed inverter required 21 switches (IGBT's) and six diode embedded bidirectional switches, but in common three phase multi-level inverter required 48 switches (IGBT's). So this topology have reduces a switching loss and high efficiency. A boost converter (step-up DC-DC) used in paper for high voltage before proposed inverter; this topology was applied to three phase asynchronous machine photovoltaic system with considerations for voltage control pulse generator.

II.   Photovoltaic System (PV)

A solar cell basically is a p-n semiconductor junction. When exposed to light, a current proportional to solar irradiance is generated. Standard simulation tools utilize the approximate diode equivalent circuit shown in Fig. 1 in order to simulate all electric circuits that contain diode. The circuit consists of R_{on} in series with voltage source V_{on}. PVs generate electric power when illuminated by sunlight or artificial light, the absorption of photons of energy greater than the band-gap energy of the semiconductor promotes electrons from the valence band to the conduction band, creating hole-electron pairs throughout the illuminated part of the semiconductor. These electrons and holes pairs will flow in opposite directions across the junction thereby creating DC power.
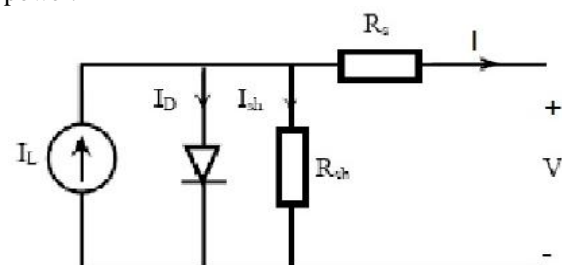

Figure 1: circuit model of PV cell.

2.1 Mathematical Model:

The equation [1] & [2] that are used to solve the mathematical model of the solar cell based on simple equivalent circuit shown in Fig. 1, are given below;

$$I_D = I_0 \left[e^{\frac{q(V+IR_s)}{KT}} - 1 \right] \qquad \text{-(1)}$$

$$I = I_L - I_0 \left[e^{\frac{q(V+IR_s)}{KT}} - 1 \right] - \frac{(V+IR_s)}{R_{sh}} \qquad \text{-(2)}$$

Where:
I is the cell current in (A).
q is the charge of electron = 1.6x10-19 (coul).
K is the Boltzmann constant (j/K).
T is the cell temperature (K).
I_L is the light generated current (A).
I_0 is the diode saturation current.
R_s , R_{sh} are cell series and shunt resistance (ohms).
V is the cell output voltage (V).

Table 1: pv module characterstics.

Model : SIEMENS SP75	
Max Power	: 75W
Short circuit current, I_{SC}	: 4.8A
MPPT current, I_{MPPT}	: 4.4 A
Open Circuit voltage, V_{OC}	: 21.7V
MPPT voltage, V_{MPPT}	: 17.0V

2.2 Comparison of Full H-Bridge and Hybrid H-Bridge inverter

2.2.1 Full H-Bridge
Fig.2 shows the Full H-Bridge Configuration. By using single H-Bridge we can get three voltage levels. The number output voltage levels of cascaded Full H-Bridge are given by 2n+1 and voltage step of each level is given by Vdc/n. Where n is number of H-bridges connected in cascaded, the switching table is given in Table 2.
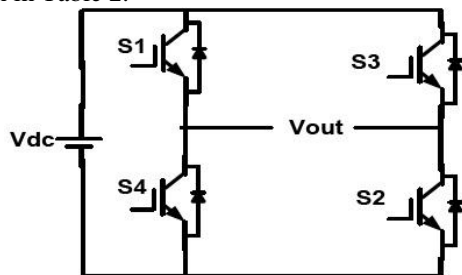

Figure 2: Full H-Bridge.

Table 2: Switching table for Full H-Bridge.

Switches Turn ON	Voltage Level
S1,S2	V_{dc}
S3,S4	$-V_{dc}$
S4,S2	0

2.2.2 Hybrid H-Bridge
Figure 3, shows the Hybrid H-Bridge configuration. By using single Hybrid H-Bridge we can get seven voltage levels. The number output voltage levels of cascaded Hybrid H-Bridge are given

by 6n+1 and voltage step of each level is given by Vdc/4n. Where n is number of H-bridges connected in cascaded, the switching table of Hybrid H-Bridge is given in Table 3.
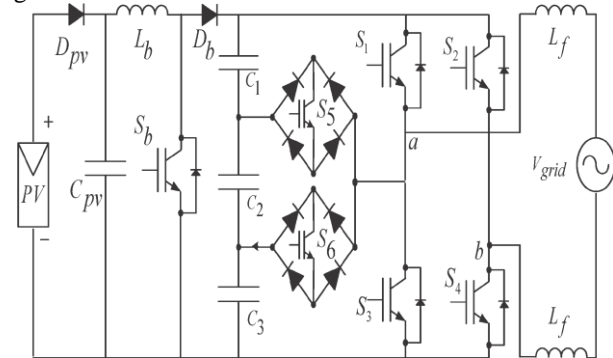

Figure 3: Single-phase proposed seven- level inverter with open loop.

Table 3: Output Voltages according to switches on-off conditions.

v_0	S_1	S_2	S_3	S_4	S_5	S_6
V_{dc}	on	off	off	on	off	off
$2V_{dc}/3$	off	off	off	on	on	off
$V_{dc}/3$	off	off	off	on	off	on
0	off	off	on	on	off	off
0*	on	on	off	off	off	off
$-V_{dc}/3$	off	on	off	off	off	off
$-2V_{dc}/3$	off	on	off	off	off	on
$-V_{dc}$	off	on	on	off	off	off

In full H-bridge inverter used four switches for three levels and hybrid H-bridge inverter used six switches for seven levels, so in hybrid inverter number of switches reduces in order to reduces switching loss.

2.3 PWM modulation
A novel PWM modulation technique was introduced to Generate the PWM switching signals. Three reference signals (*V*ref1, *V*ref2, and *V*ref3) were compared with a carrier signal (*Vcarrier*). The reference signals had the same frequency and amplitude and were in phase with an offset value that was equivalent to the amplitude of the carrier signal. The reference signals were each compared with the carrier signal. If *V*ref1 had exceeded the peak amplitude of *V*carrier, *V*ref2 was compared with *V*carrier until it had exceeded the peak amplitude of *V*carrier. Then, onward, *V*ref3 would take charge and would be compared with *V*carrier until it reached zero. Once *V*ref3 had reached zero, *V*ref2 would be compared until it reached zero. Then, onward, *V*ref1 would be compared with *V*carrier. The resulting switching pattern. Switches *S*1, *S*3, *S*5, and *S*6 would be switching at the rate of the carrier signal frequency, whereas *S*2 and *S*4 would operate at a frequency that

A R N Rao et al Int. Journal of Engineering Research and Applications
www.ijera.com
ISSN : 2248-9622, Vol. 3, Issue 6, Nov-Dec 2013, pp.2053-2059

was equivalent to the fundamental frequency. For one cycle of the fundamental frequency, the proposed inverter operated through six modes. The per unit output-voltage signal for one cycle.
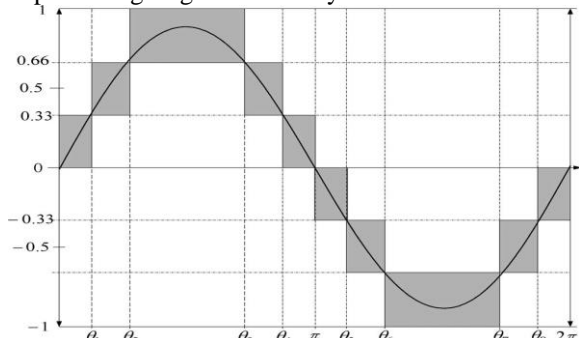

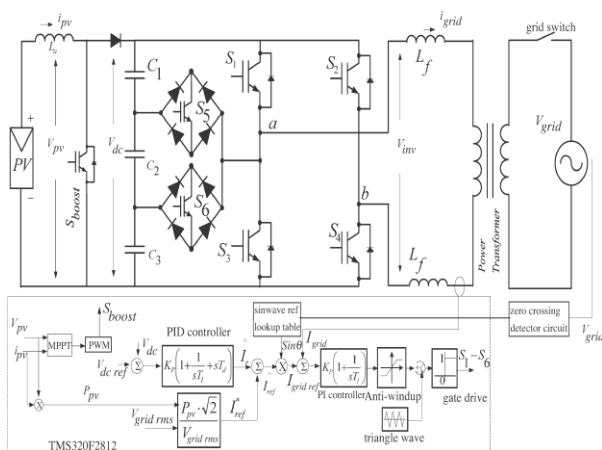Figure 4: Seven-level output voltage (Vab) and switching angles.

Figure 5: Seven-level inverter with closed-loop control algorithm

2.4 control system

The control system comprises a MPPT algorithm, a dc-bus voltage controller, reference-current generation, and a current controller. The two main tasks of the control system are maximization of the energy transferred from the PV arrays to the grid, and generation of a sinusoidal current with minimum harmonic distortion, also under the presence of grid voltage harmonics. The proposed inverter utilizes the perturb-and-observe (P&O) algorithm for its wide usage in MPPT owing to its simple structure and requirement of only a few measured parameters. It periodically perturbs (i.e., increment or decrement) the array terminal voltage and compares the PV output power with that of the previous perturbation cycle. If the power was increasing, the perturbation would continue in the same direction in the next cycle; otherwise, the direction would be reversed. This means that the array terminal voltage is perturbed every MPPT cycle; therefore, when the MPP is reached, the P&O algorithm will oscillate around it. The P&O algorithm was implemented in the dc–dc boost converter. The output of the MPPT is the duty-cycle function. As the dc-link voltage Vdc was controlled in the dc–ac seven level PWM inverter; the

change of the duty cycle changes the voltage at the output of the PV panels. A PID controller was implemented to keep the output voltage of the dc–dc boost converter (Vdc) constant by comparing Vdc and Vdc ref and feeding the error into the PID controller, which subsequently tries to reduce the error. In this way, the Vdc can be maintained.
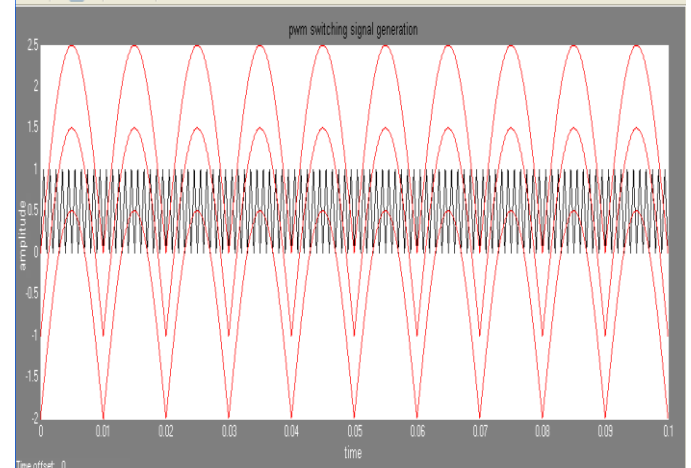

Figure 6: Simulation of pwm switching sequence.

For *Ma* that is equal to, or less than, 0.33, only the lower reference wave (Vref3) is compared with the triangular carrier signal. The inverter's behaviour is similar to that of a conventional full-bridge three-level PWM inverter. However, if *Ma* is more than 0.33 and less than 0.66, only Vref2 and Vref3 reference signals are compared with the triangular carrier wave. The output voltage consists of five dc-voltage levels. The modulation index is set to be more than 0.66 for seven levels of output voltage to be produced. Three reference signals have to be compared with the triangular carrier signal to produce switching signals for the switches.
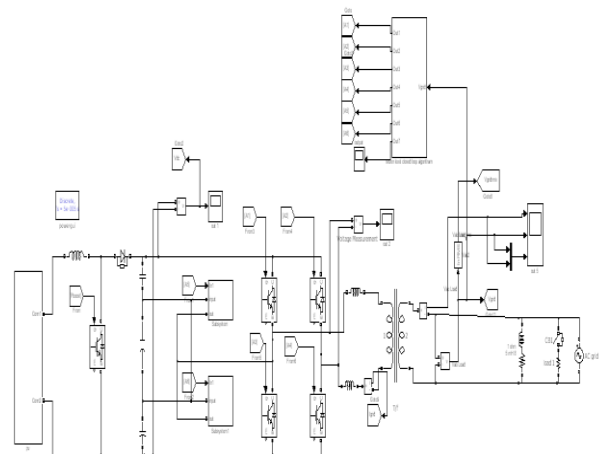

Figure 7: Simulation circuit of Seven-level inverter with closed-loop control algorithm

III. Single-Phase Proposed Inverter

The proposed single-phase nine-level inverter was developed from the five-level inverter in [12]. It comprises a single-phase conventional H-bridge

A R N Rao et al Int. Journal of Engineering Research and Applications
www.ijera.com
ISSN : 2248-9622, Vol. 3, Issue 6, Nov-Dec 2013, pp.2053-2059

inverter, three bidirectional switches, and a capacitor voltage divider formed by *C*, as shown in Figure. 8. The modified H-bridge topology is significantly advantageous over other topologies, i.e., less power switch, power diodes, and less capacitor for inverters of the same number of levels. Photovoltaic (PV) arrays were connected to the inverter via a dc–dc boost converter. The power generated by the inverter is to be delivered to the power network, so the utility grid, rather than a load, was used. The dc–dc boost converter was required because the PV arrays had a voltage that was lower than the three phase induction motor rating.

Figure 8: Single-phase proposed Nine- level inverter with open loop.

High dc bus voltages are necessary to ensure that power flows from the PV arrays to electrical machine. Proper switching of the inverter can produce seven output-voltage levels (V_{dc}, $3V_{dc}/4$, $Vdc/2$, $V_{dc}/4$, 0, $-V_{dc}/4$, $-V_{dc}/2$, $-3V_{dc}/4$, $-V_{dc}$) from the dc supply voltage.

Table 4: Output Voltages according to switches on-off conditions.

V_0	S_1	S_2	S_3	S_4	S_5	S_6	S_7
V_{dc}	on	off	off	on	off	off	off
$\frac{3V_{dc}}{4}$	off	off	off	on	on	off	off
$\frac{V_{dc}}{2}$	off	off	off	on	off	on	off
$\frac{V_{dc}}{4}$	off	off	off	on	off	off	on
0	off	off	on	on	off	off	off
0*	on	on	off	off	off	off	off
$\frac{-V_{dc}}{4}$	off	on	off	off	on	off	off
$\frac{-V_{dc}}{2}$	off	on	off	off	off	on	off
$\frac{-3V_{dc}}{4}$	off	on	off	off	off	off	on
$-V_{dc}$	off	on	on	off	off	off	off

Zero output can be produced by two switching combinations; switches *S*3 and *S*4 are ON, or *S*1 and *S*2 are ON, and all other controlled switches are OFF; terminal *ab* is a short circuit, and the voltage applied to the load terminals is zero.
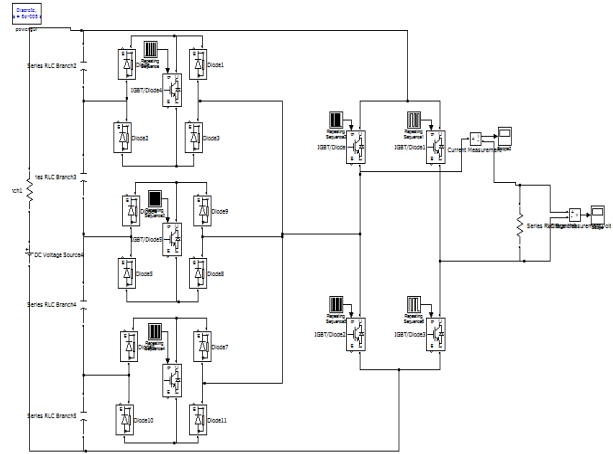

Figure 9: simulation circuit of Single-phase proposed Nine- level inverter with open loop.

3.1 Proposed Three-Phase Nine-level Inverter with Induction Motor
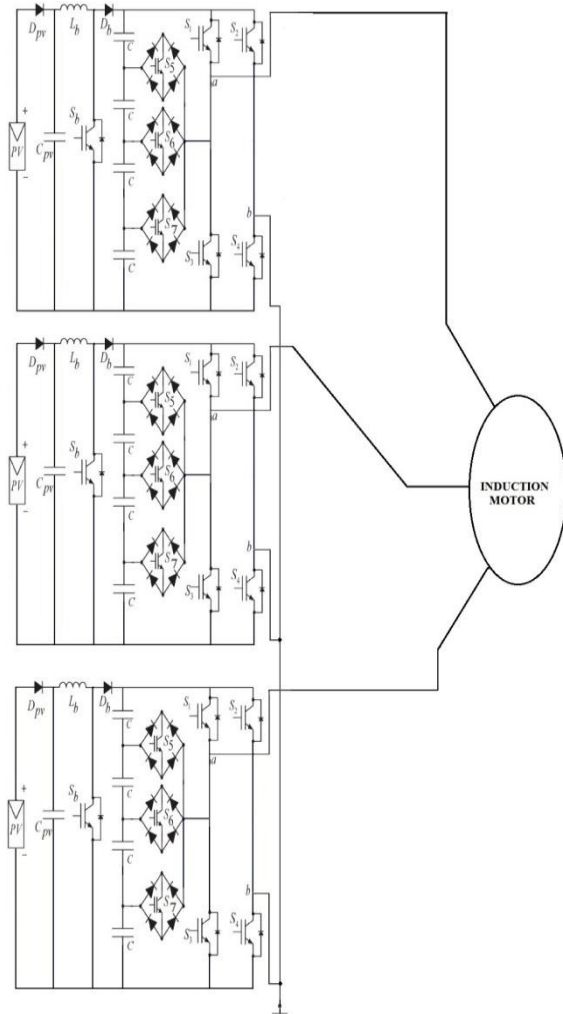

Figure 10: Three-phase nine level proposed inverter with induction motor.

Three-phase proposed nine level inverter connected in single phase of nine level inverters electrically placed and operated by 120^0. As shown in

figure.10. Three-phase nine levels proposed inverter with induction motor. Three phase induction motors are used in many applications at same time the speed control technique easy and high efficiency. This proposed inverter switches can be controlled by triggering pulse according to the output voltages conditions. The proposed inverter repeating sequence is applied in each switch depends on switching sequence and output voltage.
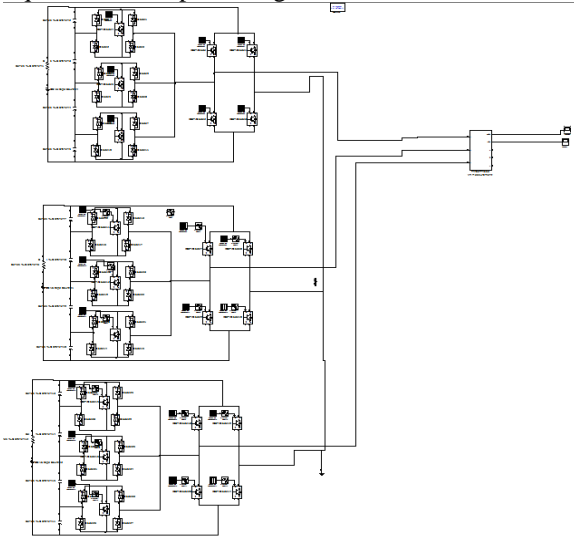

Figure 11: simulation circuit of three-phase nine-level proposed inverter with induction motor.

3.2 Induction Motor

In recent years the control of high-performance induction motor drives for general industry applications and production automation has received widespread research interests. Induction machine modelling has continuously attracted the attention of researchers not only because such machines are made and used in largest numbers but also due to their varied modes of operation both under steady and dynamic states. Three phase induction motors are commonly used in many industries and they have three phase stator and rotor windings. The stator windings are supplied with balanced three phase ac voltages, which produce induced voltages in the rotor windings due to transformer action. It is possible to arrange the distribution of stator windings so that there is an effect of multiple poles, producing several cycles of magneto motive force (mmf) around the air gap. This field establishes a spatially distributed sinusoidal flux density in the air gap.

In this paper three phase induction motor as a load. The equivalent circuit for one phase of the rotor is shown in figure. 12.
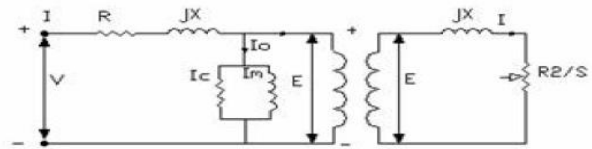

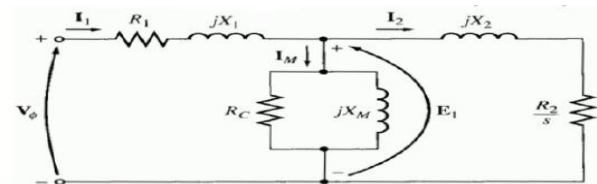Figure 12: Steady state equivalent circuit of induction motor.

Figure 13: Equivalent circuit refers to stator side.
The rotor current is

$$I_r = \frac{sE_r}{R_r + jX_r}$$
$$= \frac{E_r}{\frac{R_r}{s} + jX_r}$$

The complete circuit model with all parameters referred to the stator is in figure. 13. Where Rs and Xs are per phase resistance and leakage reactance of the stator winding. Xm represents the magnetizing reactance. R'r and X'r are the rotor resistance and reactance referred to the stator. I'r is the rotor current referred to the stator. There will be stator core loss, when the supply is connected and the rotor core loss depends on the slip.

IV. Simulation and results of proposed concept

MATLAB SIMULINK simulated the proposed three phase inverter fed to induction motor as shown in figure 14.
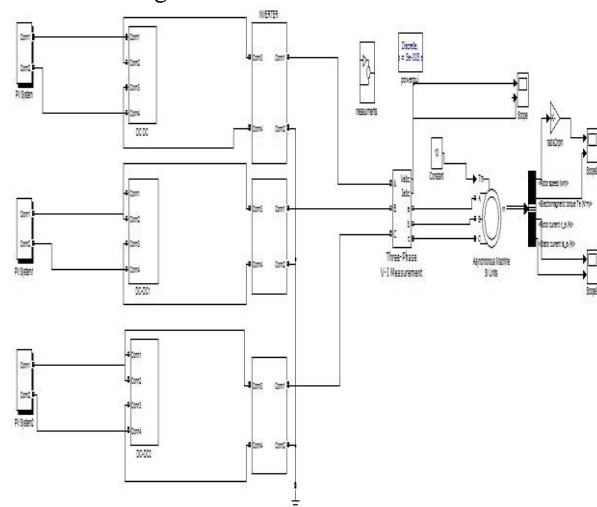

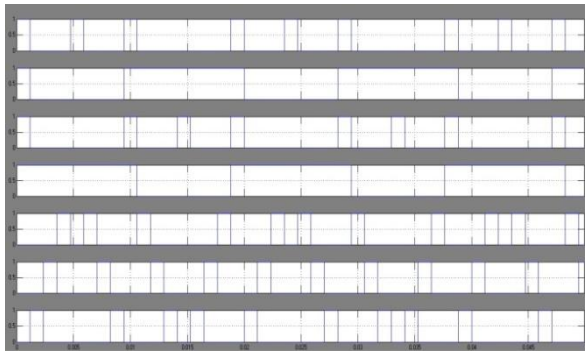Figure 14: MATLAB/SIMULINK model of three phase nine-level proposed inverter fed to induction motor.

Figure 15: Switching pulses for nine-level inverter.

In proposed inverter before placed a boost dc-dc converter operated with frequency f_b = 10KHz.which is step up the output voltage of PV panel up to 400V and PV output voltage is 50V. This PV voltage depended on solar radiation which is simulated as figure.1 each phase have separate PV panel and boost dc-dc converter. Three phase proposed nine inverter switching pulse per phase shown in figure 17. Remaining two phase switching control pulse operated with displacement of120^0.
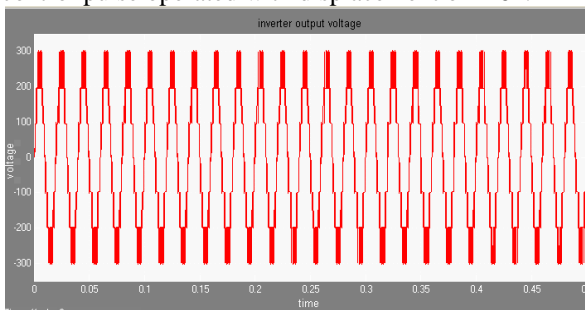

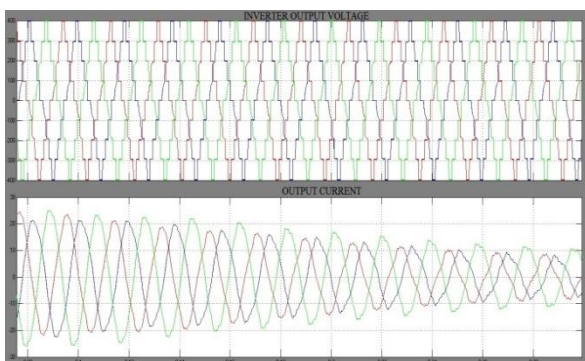Figure 16: single-phase seven-level inverter output voltage

Figure 17: Three-phase nine-level inverter (a) Output Voltage, (b) Output Current.
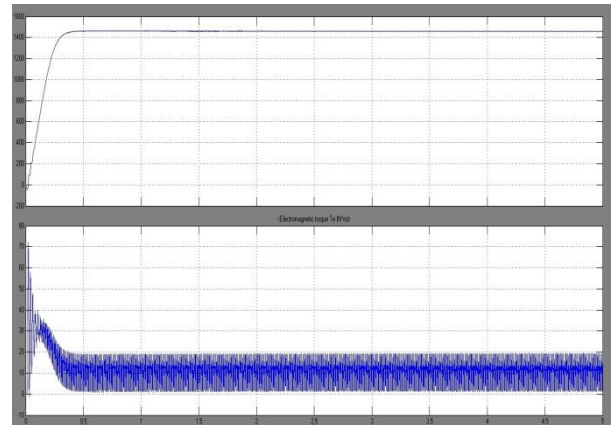

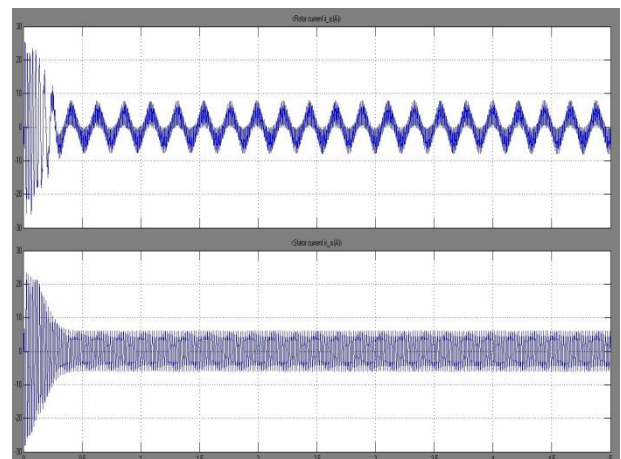Figure 18: Induction Motor (a) Rotor speed, (b) Electromagnetic Torque.

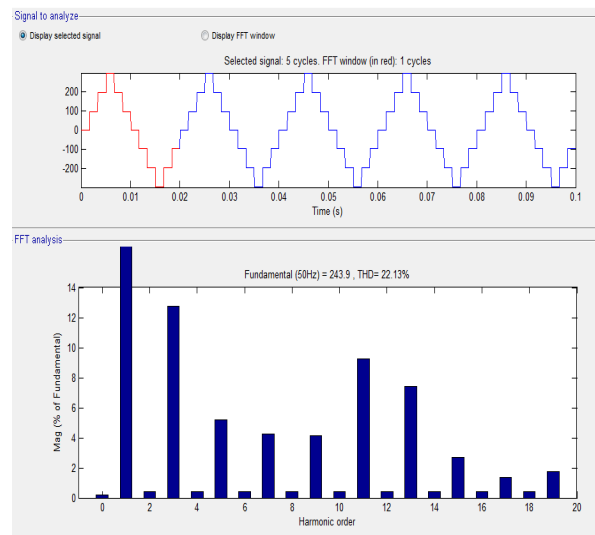Figure 19: Induction motor (a) Rotor current, (b) stator current.

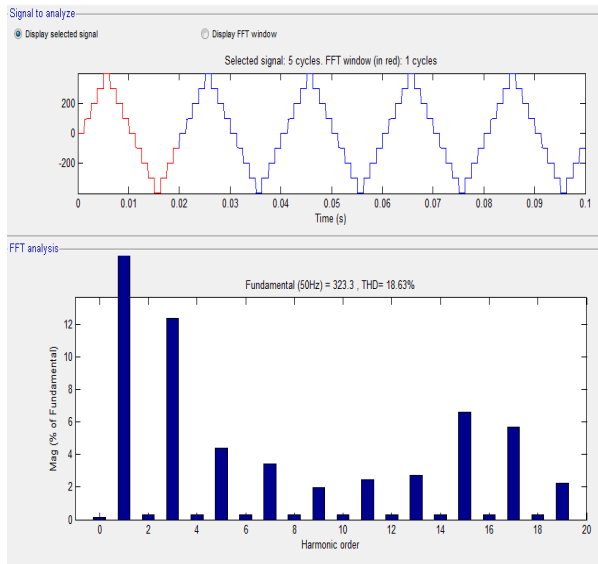Figure 20: THD result for seven-levels of output voltage

Figure 21: THD result for nine-levels of output voltage.

The THD measurement of Fig.19 corresponds to the waveform of Fig. 20, while the THD measurements correspond to the waveforms of respectively. Comparing all two THD measurements, the nine-level inverter produced the lowest THD compared with the seven-level inverter. This proves that, as the level increases, the THD reduces.

Table5: total harmonic distortion different levels

Inverter level	THD
Seven level	22.13%
Nine level	18.63%

Three phase nine-level inverter output voltage and current as shown in figure 17. This proposed inverter output applied to induction motor of rating is 400V, 50Hz, below 1500RPM, and load torque 10. Induction motor results shown in figure 18 and 19, in figure 18 shown rotor speed 1460RPM and Electromagnetic torque; in figure 19 shown rotor current and stator current. Finally THD in circuit 18%, this proposed topology is very high efficiency and economic.

V. Conclusion

This paper presents a new three phase nine-level inverter with reduced switches compare to common multi level inverter. Multilevel inverters offer improved output waveforms and lower THD. In this topology less THD in the nine-level inverter compared with that in the seven-level inverters is connected PV inverters. This inverter provided to induction motor with smooth output and better voltage. Switching loss reduce in this topology than the common three phase multi-level-inverter.

References

[1] M. Calais and V. G. Agelidis, "Multilevel converters for single-phase grid connected photovoltaic systems—An overview," in *Proc.*

IEEE Int. Symp. Ind. Electron., 1998, vol. 1, pp. 224–229.

[2] S. B. Kjaer, J. K. Pedersen, and F. Blaabjerg, "A review of single-phase grid connected inverters for photovoltaic modules," *IEEE Trans. Ind. Appl.*, vol. 41, no. 5, pp. 1292–1306, Sep./Oct. 2005.

[3] P. K. Hinga, T. Ohnishi, and T. Suzuki, "A new PWM inverter for photovoltaic power generation system," in *Conf. Rec. IEEE Power Electron. Spec. Conf.*, 1994, pp. 391–395.

[4] Y. Cheng, C. Qian, M. L. Crow, S. Pekarek, and S. Atcitty, "A comparison of diode-clamped and cascaded multilevel converters for a STATCOM with energy storage," *IEEE Trans. Ind. Electron.*, vol. 53, no. 5, pp. 1512–1521, Oct. 2006.

[5] M. Saeedifard, R. Iravani, and J. Pou, "A space vector modulation strategy for a back-to-back five-level HVDC converter system," *IEEE Trans. Ind. Electron.*, vol. 56, no. 2, pp. 452–466, Feb. 2009.

[6] S. Alepuz, S. Busquets-Monge, J. Bordonau, J. A. M. Velasco, C. A. Silva, J. Pontt, and J. Rodríguez, "Control strategies based on symmetrical components for grid-connected converters under voltage dips," *IEEE Trans. Ind. Electron.*, vol. 56, no. 6, pp. 2162–2173, Jun. 2009.

[7] J. Rodríguez, J. S. Lai, and F. Z. Peng, "Multilevel inverters: A survey of topologies, controls, and applications," *IEEE Trans. Ind. Electron.*, vol. 49, no. 4, pp. 724–738, Aug. 2002.

[8] J. Rodriguez, S. Bernet, B. Wu, J. O. Pontt, and S. Kouro, "Multilevel voltage-source-converter topologies for industrial medium-voltage drives," *IEEE Trans. Ind. Electron.*, vol. 54, no. 6, pp. 2930–2945, Dec. 2007.

[9] M. M. Renge and H. M. Suryawanshi, "Five-level diode clamped inverterto eliminate common mode voltage and reduce dv/dt in medium voltagerating induction motor drives," *IEEE Trans. Power Electron.*, vol. 23, no. 4, pp. 1598–1160, Jul. 2008.

[10] E. Ozdemir, S. Ozdemir, and L. M. Tolbert, "Fundamental-frequencymodulatedsix-level diode-clamped multilevel inverter for three-phasestand-alone photovoltaic system," *IEEE Trans. Ind. Electron.*, vol. 56, no. 11, pp. 4407–4415, Nov. 2009.

[11] P. Lezana, R. Aguilera, and D. E. Quevedo, "Model predictive controlof an asymmetric flying capacitor converter," *IEEE Trans. Ind. Electron.*, vol. 56, no. 6, pp. 1839–1846, Jun. 2009.

[12] G. Ceglia, V. Guzman, C. Sanchez, F. Ibanez, J. Walter, and M. I. Gimanez, "A new simplified multilevel inverter topology for DC–AC conversion," *IEEE Trans. Power Electron.*, vol. 21, no. 5, pp. 1311–1319, Sep. 2006.